Fusion Engineering and Design 218 (2025) 115139

Contents lists available at ScienceDirect

Fusion Engineering and Design

journal homepage: www.elsevier.com/locate/fusengdes

Preliminary thermomechanical assessment of the prototypical mock-up of the DEMO WCLL first wall to be tested in the Water Loop facility

F.M. Castrovinci [a,*], P. Arena [a], N. Badodi [a], G. Bongiovì [b], I. Catanzaro [b], A. Del Nevo [a], P.A. Di Maio [b], S. Giambrone [b], P. Maccari [a], G. Mongiardini [c], A. Quartararo [b], E. Vallone [b]

[a] ENEA NUC-ING C. R. Brasimone, 40032 Camugnano, Bologna, Italy
[b] Department of Engineering, University of Palermo, Viale delle Scienze, Ed. 6, 90128 Palermo, Italy
[c] DIAEE Department, Sapienza University of Rome, 00186, Roma, Italy

ARTICLE INFO

Keywords:
DEMO
Breeding blanket
Prototypical mock-up

ABSTRACT

The Water-thermalHYDRAulic (W-HYDRA) experimental platform, under construction at the ENEA Brasimone research centre, has the main goal of testing and validating the technologies to be adopted for the EU-DEMO Water Cooled Lead Lithium (WCLL) Breeding Blanket (BB) and its ancillary systems. One of the W-HYDRA facilities is the Water Loop (WL), a mid-scale facility capable of supplying water at Pressurized Water Reactor conditions to test the EU-DEMO BB mock-ups and ITER's WCLL Test Blanket Module to carry out experimental activities aimed at validating numerical codes and safety procedures. In this framework, the present work deals with the preliminary study of the thermomechanical behaviour of a Prototypical Mock-Up (PMU) of the WCLL BB First Wall (FW), in sight of its design optimization and the related experimental campaigns in the WL facility. The assessment of the FW PMU's structural performances was carried out, allowing the investigation of its global response under the load combinations foreseen for the tests and verifying the fulfilment of the RCC-MRx structural design rules. The thermal field adopted for the thermomechanical simulation was calculated by dedicated coupled fluid–structure Computational Fluid-Dynamic analysis and the FW PMU cooling performances were addressed as well. The work was carried out following a theoretical–numerical approach based on the finite volume method and on the finite element method, adopting the ANSYS CFX and ANSYS Mechanical commercial codes. This work presents and discusses the obtained results, along with models, loads and boundary conditions.

1. Introduction

The BB is a key in-vessel system of the DEMO fusion reactor. Due to its complex layout and to the expected severe working conditions, some design issues have to be addressed via experimental campaigns [1]. These experiments are crucial to assess the thermal-hydraulic and thermomechanical performances of BB components and their potential showstoppers. Moreover, they will provide sets of experimental data broad enough to validate the computational methodologies so far adopted for the DEMO design, allowing to properly adjust the conservative approach followed in the numerical analyses [2–6]. To this end, the W-HYDRA experimental platform is being built at the ENEA Brasimone research centre, with the main goal of testing and validating the technologies to be adopted for the WCLL BB and its ancillary systems [7]. In particular, one of the milestones of the project is the design of a Prototypical Mock-Up (PMU) of the WCLL BB FW and its experimental test on the Water Loop (WL) facility, integrated in the W-HYDRA platform.

The objective of the present work, framed within the Work Package BB of the EUROfusion action, is the preliminary assessment of the thermomechanical behaviour of the FW PMU test section, along with the study of the circuit cooling capabilities and its thermal behaviour. This evaluation aims at providing insights that will help optimizing the design of the test section to obtain a reliable design of the component, needed to assure the structural integrity for the required lifetime.

Therefore, a thermofluid-dynamic and thermomechanical analysis campaign was performed. In particular, at first, the FW PMU cooling performances and the assessment of the structural thermal field of the test section to be adopted for the thermomechanical analysis were addressed by means of Computational Fluid Dynamic (CFD) calculations. Then, the study of the FW PMU's structural behaviour was carried out, allowing the investigation of its global response under the load

* Corresponding author.
E-mail address: francesca.castrovinci@enea.it (F.M. Castrovinci).

https://doi.org/10.1016/j.fusengdes.2025.115139
Received 16 January 2025; Received in revised form 26 March 2025; Accepted 28 April 2025

Table 1
Summary of FW PMU cooling circuit design parameters.

PMU thickness	25 mm + 2 mm
PMU length	1575 mm
PMU height	180 mm
Channel pitch	22.5 mm
Manifolds diameters	3/8" – 2"
Number of cooling channels	8
Operating pressure	155 bar
Inlet temperature	295 °C

combination foreseen for the experimental test, in terms of equivalent stress and displacement fields. Moreover, results were compared with the RCC-MRx structural design criteria to ensure their compliance with the standards [8].

2. The WCLL breeding blanket first wall prototypical mock-up

The FW of the WCLL BB concept consists of a steel structure, cooled by C-shaped squared water channels. It is going to be made of EUROFER97 steel with a 2 mm layer of Tungsten on the plasma-facing surface [9]. A WCLL BB FW PMU will be tested at ENEA Brasimone labs on the WL facility, which will provide pressurized water at Pressurized Water Reactor (PWR) conditions.

The reference FW PMU design was based on the FW geometry of the Central Outboard Blanket (COB) segment and subjected to the thermal loads of the COB elementary cell at the equatorial level, under normal operating conditions [10]. It consists of a 4-channel configuration with a 33.75 mm channel pitch.

Recently, both COB equatorial level and O7 level (COB-O7) elementary cells, whose locations are reported in Fig. 1 were studied, adopting the thermal loads relevant to the COB-O7. These loads present a lower nuclear heating (which cannot be experimentally reproduced for the FW PMU) and higher heat flux, compared to the loads to which the COB equatorial level is subjected, under normal operating conditions. As an outcome of the study, the COB-O7 layout (Fig. 2), consisting of a 6-channels configuration with a channel pitch of 22.5 mm was chosen as a reference configuration for the design of the FW PMU, showing the most representative cooling conditions and thermal behaviour under the COB-O7 thermal loads [11,12].

The CAD model of the FW PMU test section is depicted in Fig. 3. The FW PMU is designed as a plate that represents the front part of the WCLL BB FW and its length includes the flat toroidal section and the two elbows. The PMU material will be chosen to closely match the properties of EUROFER97 steel [13] (e.g., martensitic steel, if EUROFER97 will not be available). In order to reproduce the heat flux deposited on the WCLL BB FW and study the related heat transfer phenomena, the FW PMU test section will be placed inside a Vacuum Chamber (VC) connected to the WL. The VC will be equipped with an 800 kW Electron Beam (EB) gun able to deliver high heat fluxes on the FW PMU and it will be installed on one of the two side flanges of the VC [7].

The layout of the FW PMU cooling circuit replicates 8 channels with countercurrent cooling path. The FW PMU test section will be connected to the WL via AISI316 piping. In this configuration, water will enter the system through an inlet manifold, and it will be sent to two distributors, each feeding 4 FW PMU square channels. After exiting the PMU, the coolant will flow inside two collectors, and from there it will be directed to the outlet manifold of the VC. The main design parameters and the operating conditions are summarized in Table 1.

The thermofluid-dynamic and thermomechanical behaviour of the considered FW PMU test section were assessed assuming the coolant operative conditions of Table 1, being the same of the WCLL BB FW, and the reference heat loads foreseen for the WCLL BB segment of the COB-O7, which will be adopted in the flat top conditions of the experimental tests.

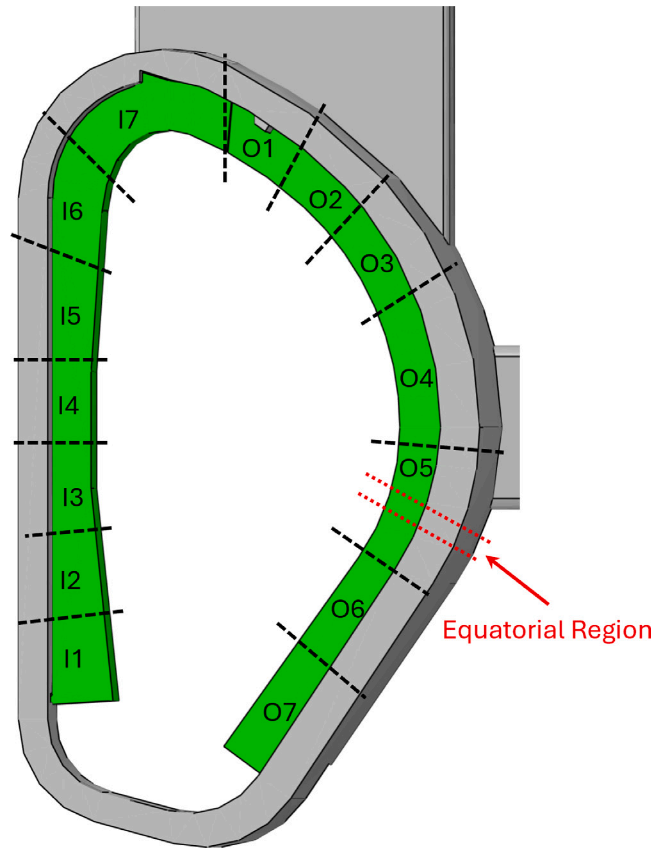

Fig. 1. Poloidal section of the DEMO BB and nomenclature of the Inboard and Outboard segments.

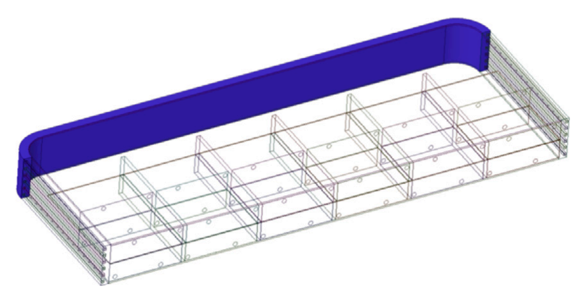

Fig. 2. FW of the EU-DEMO WCLL concept.

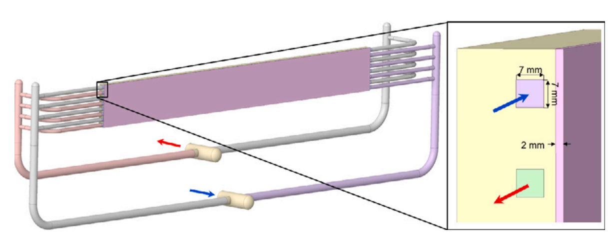

Fig. 3. FW PMU test section CAD model.

3. Thermofluid-dynamic analyses

A thermofluid-dynamic research campaign was carried out on the actual design of the FW PMU test section to study the circuit cooling capabilities and its thermal behaviour, to highlight the possible occurrence of hot spots and potential water vaporization issues.

Table 2
FW PMU mesh parameters.

	Coolant	Structure
Mesh type	Hybrid structured/Unstructured	
Nodes	3 014 904	6 896 232
Elements	3 508 974	30 963 341
Number of inflation layers	16	–
First layer thickness [μm]	7 10	–
Layers growth rate	1.3	–
Element size [mm]	0.7–5	1–5

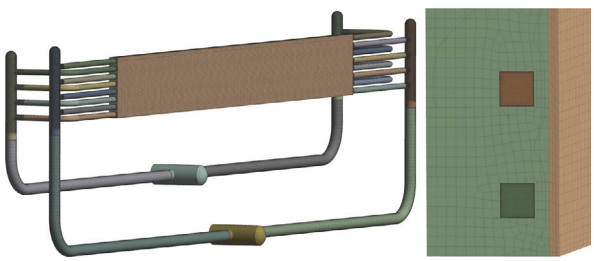

Fig. 4. FW PMU model discretization.

A fully coupled fluid–structure 3D-CFD analysis campaign was performed aiming at evaluating:

- the coolant total pressure distribution and overall total pressure drop;
- the coolant flow velocity distribution among the FW PMU cooling channels;
- the coolant temperature distribution;
- the distribution of margin against saturation in the coolant;
- the thermal behaviour of the structures.

The thermal-hydraulic behaviour of the FW PMU cooling circuits was assessed following a numerical approach based on the Finite Volume Method and adopting the ANSYS-CFX 2021 R2 commercial CFD code [14].

3.1. CFD analyses setup

The CAD model adopted for the simulation including fluid and structure domain is reported in Fig. 3.

The calculation grid adopted for the simulation was composed of approximately 33 million of elements and 10 million nodes. More details of the assembled mesh set up for the CFD analysis are reported in Fig. 4, while its main parameters are depicted in Table 2.

The CFD analyses of the FW PMU were performed adopting the setup and the operative conditions of Table 3.

The complete simulation was carried out considering the FW PMU coolant at PWR conditions, i.e. an inlet pressure of 155 bar and an inlet temperature of 295 °C. Moreover, a total Mass Flow Rate (MFR) of 1.048 kg/s was adopted to be representative of the COB-O7 FW.

Considering the thermal loads, the FW PMU is supposed to operate with a maximum heat flux of 0.6616 MW/m^2 on the front surface, heated up by the EB gun and a constant heat flux of 90 kW/m^2 on the back surface, provided by a system of electrical heaters. The heat flux distribution on the front surface of the FW PMU is reported in Fig. 5.

Moreover, the front surface is simulated with a uniform heat flux equal to its maximum value for the overall length corresponding to the WCLL BB FW length. Considering the length corresponding to the WCLL FW elbows, the heat flux will follow a sinusoidal profile, as in [10], approaching zero at the borders. These values are estimated considering as reference the heat loads foreseen for the COB-O7 of the WCLL BB, taking into account the heat flux from the plasma, the neutronic power and the heat exchange with the Breeding Zone [10].

Table 3
Model setup and operative conditions.

Analysis type	Steady-State coupled
Fluid	Water IAPWS IF97 [15]
Structure	EUROFER97 [13]
	AISI316 [16]
FW heat flux (Max)	0.6616 MW/m^2
Back surface heat flux	0.090 MW/m^2
Turbulence model	k-ω SST
Boundary layer model	Automatic wall functions
Wall absolute roughness	15 μm
Inlet BC (T/p)	295 °C/15.5 MPa
Outlet BC (MFR)	1.048 kg/s

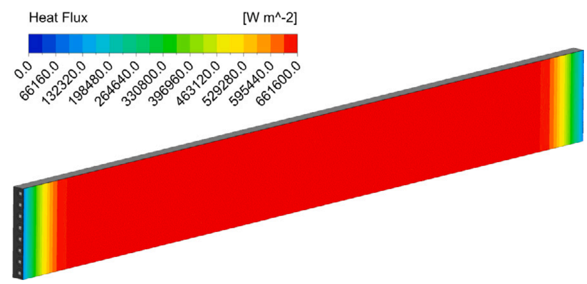

Fig. 5. PMU FW heat flux distribution.

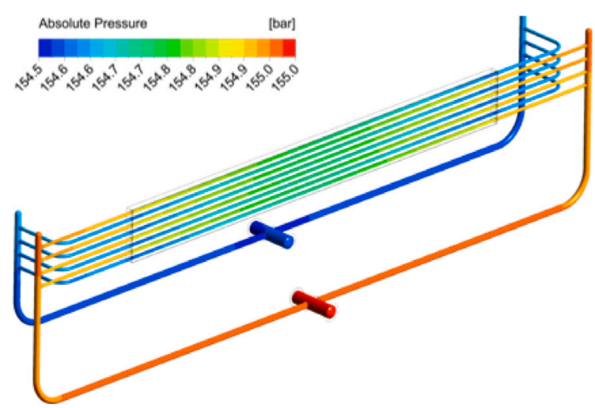

Fig. 6. FW PMU absolute pressure distribution.

Table 4
Coolant axial flow velocity distributions main parameters.

Maximum velocity [m/s]	3.850
Minimum velocity [m/s]	3.823
ϵ	0.69%
Average velocity [m/s]	3.837
σ [m/s]	0.009
CV	0.23%

3.2. Results

The absolute pressure distribution is reported in Fig. 6. The test section total pressure drop amounts to 0.45 bar. It should be noted that this result does not reflect the phase-change model in the analysis for which further research is needed.

The main parameters regarding the coolant axial velocity distribution among the FW PMU channels are reported in Table 4. In particular, they are the standard deviation σ, the relative span ϵ and the Coefficient of Variation (CV), which is defined as the ratio between the standard deviation and the average value of the considered data set.

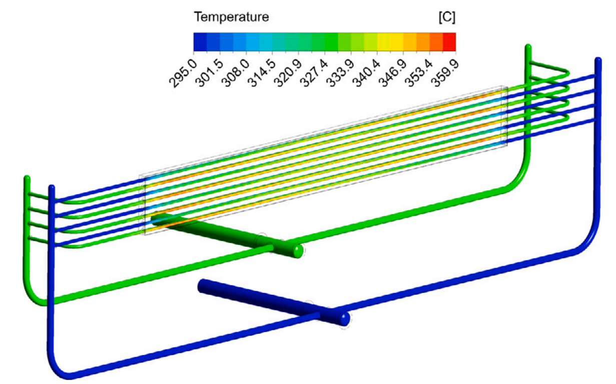

Fig. 7. Coolant temperature distribution among the test section cooling circuit.

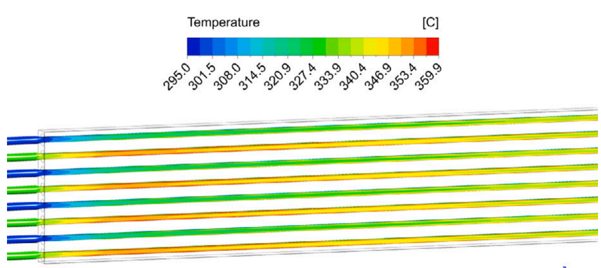

Fig. 8. Coolant temperature distribution among the FW channels.

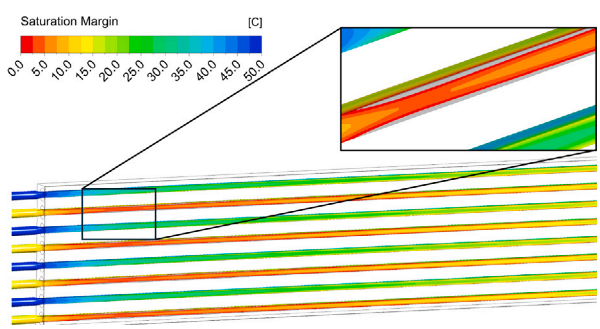

Fig. 9. Saturation margin distribution among the FW channels.

From the results, it is possible to argue that the axial flow velocity distribution is uniform among the eight FW channels with negligible differences (maximum deviations lower than 1%).

In order to check whether these balanced coolant flow distributions might ensure a proper cooling of the FW PMU structure, coolant temperature distribution and coolant margin against saturation were considered.

The coolant temperature distribution is reported in Fig. 7 and more in detail in Fig. 8. In addition, the coolant margin against saturation, defined as the difference between the saturation temperature $T_{sat}(p)$ and the local coolant temperature, with $T_{sat}(p)$ drawn from [17], is reported in Fig. 9. Regarding the Figs. 8 and 9, only half of the FW channel arrangement is reported since they present a symmetrical distribution. Moreover, in Fig. 9, the areas where the margin against saturation is lower than zero are coloured in grey.

From the results, it is possible to notice that minimum saturation margins slightly lower than zero occur on the front side, in the proximity of the outlet sections of the FW PMU square channels. This occurs right before the FW PMU sections corresponding to the WCLL FW elbows, where both the fluid and the structure reach their maximum temperatures, due to the heat flux to which the front surface is subjected. A preliminary assessment of the Critical Heat Flux (CHF) margin was carried out to check the possibility of thermal crisis. In particular, the Tong-75 correlation [18] was adopted for the calculation of the CHF within the FW channels, obtaining minimum values of CHF margin equal to 5. Therefore, it is possible to argue that there is no risk of thermal crisis within the FW channels. Nevertheless, in some limited areas of the channel, subcooled nucleate boiling may be the dominant heat transfer phenomenon, which is going to be further investigated by means of future two-phase flow calculations.

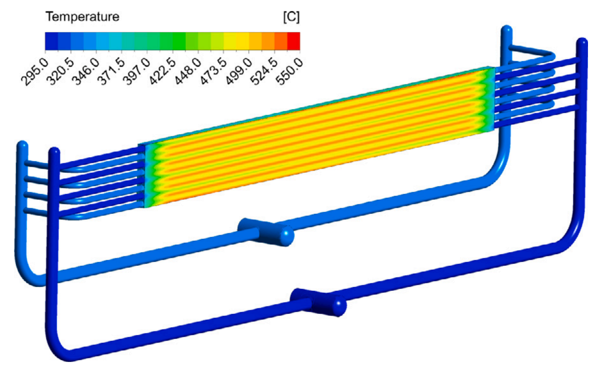

Fig. 10. Thermal field on FW PMU structure.

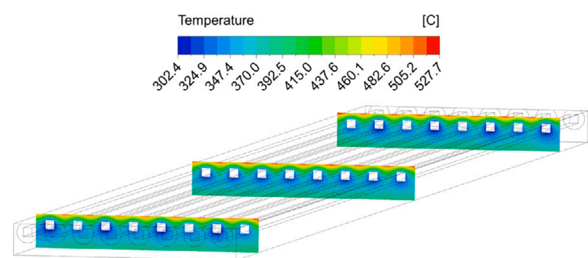

Fig. 11. Temperature distributions in three FW sections.

The structural thermal field of the PMU structure was applied to evaluate the secondary loads in the thermomechanical analyses. The temperature distribution on the overall test section structure is reported in Fig. 10 while the distribution in three sections of the FW PMU is reported in Fig. 11. The maximum temperature on the PMU structure reaches a high value, equal to about 528 °C, but within the recommended limit of 550 °C for EUROFER97 [9].

Furthermore, another loading scenario was investigated in order to obtain a structural thermal field at initial time of the operation. In this case, the same setup of Table 3 was adopted but the heat loads on the front and back surfaces were suppressed, reproducing a condition in which the EB gun and the back heaters are shut off. In particular, the back surface was considered adiabatic, while on the front surface, a simplified radiative heat transfer condition towards the VC was considered. A radiative heat flux was imposed on the surface, supposing the VC at 40 °C [19], the emissivity of the EUROFER97 equal to 0.3 and a view factor equal to 1.

The temperature distribution obtained is shown in Fig. 12. From the figure, it is possible to notice that the overall structure temperature slightly changes with respect to the inlet temperature of the fluid. The temperature field obtained on the structure was adopted to evaluate the equivalent primary and secondary stresses at the initial time of the experiments. These stress results were needed for the verification of the ratcheting criterion, which will be explained in detail in the next chapter.

4. Thermomechanical assessment

The assessment of the FW PMU structural performances was addressed, focussing on its global response, in terms of equivalent stress

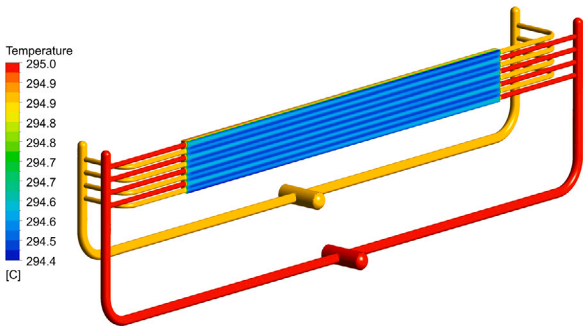

Fig. 12. Thermal field on FW PMU structure at the initial time.

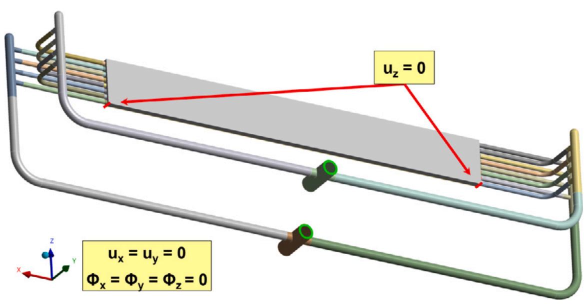

Fig. 13. FW PMU structure constraints.

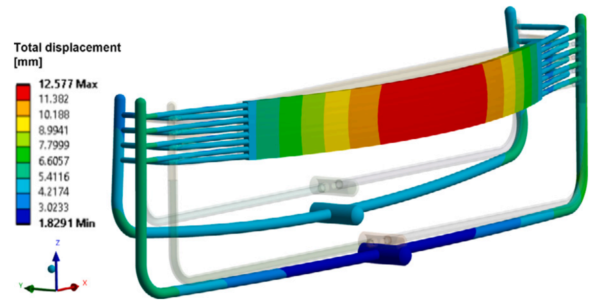

Fig. 14. FW PMU total displacement field (deformed vs. undeformed shapes).

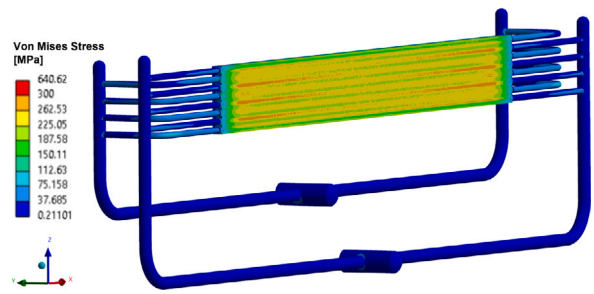

Fig. 15. FW PMU Von Mises stress field.

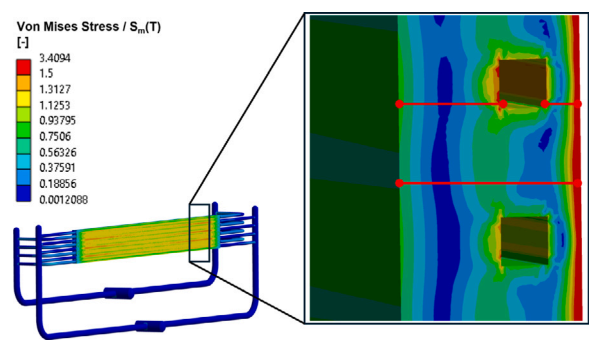

Fig. 16. Path selection within the locations A and B.

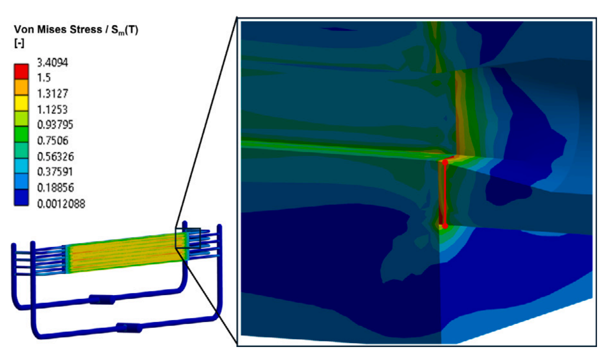

Fig. 17. Path selection within the locations C and D.

and displacement fields. Moreover, a stress linearization procedure was carried out along some significant paths in order to verify the design criteria of RCC-MRx structural code [8].

The analyses were carried out considering a steady-state flat top experimental scenario. Such testing condition mimics a normal operating condition and, according to the RCC-MRx, the service Level A of the design rules was taken into account.

The study was performed following a numerical approach based on the Finite Element Method (FEM) and adopting the ANSYS Mechanical 2021 R2 code [14].

4.1. FEM analysis setup

The preliminary structural assessment of the FW PMU test section was carried out considering the following assumptions and boundary conditions:

- the nonuniform thermal fields calculated by means of CFD analysis (Section 3.1) were imported in the model;
- a preliminary set of mechanical restraints was adopted;
- an operational pressure of 155 bar was set on the internal wall to simulate the coolant.

In particular, considering the mechanical restraints, which are depicted in Fig. 13, the displacement along the Z direction on the lower edges of the PMU was prevented. Moreover, the displacements along the X and Y directions were constrained on the faces connecting the FW PMU piping to the VC (in green in Fig. 13). On these faces, the rotations around the three axes were constrained as well.

The calculation grid adopted for the simulation was composed of approximately 10 million of nodes and 2 million of quadratic hexahedral and tetrahedral elements with a size of 1.5 mm.

4.2. Preliminary results

The preliminary structural assessment of the FW PMU test section was carried out considering the model setup described in Section 4.1.

The total displacement stress field is depicted in Fig. 14, reporting both deformed and undeformed shapes, with an amplification factor of 2x.

Looking at Fig. 14, the maximum displacement value is equal to 12.6 mm and occurs in the negative Y direction. This is probably due to the preliminary set of constraints imposed to the model and it is going

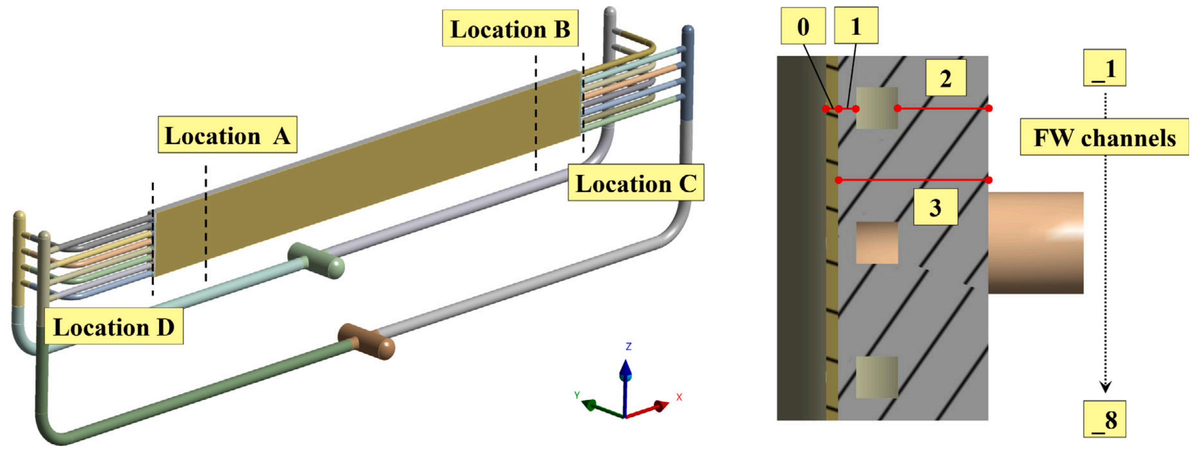

Fig. 18. Path locations nomenclature (left) and paths names for locations A and B (right).

Table 5
Design criteria.

Damage type	Criterion
Immediate excessive deformation	$\frac{P_m}{S_m} < 1$
Immediate plastic instability	$\frac{P_m+P_b}{K_{eff}S_m} < 1$
Ratcheting ($3S_m$ rule)	$\frac{(P_m+P_b)_{Max}+\Delta(P+Q)_{Max}}{3S_m} < 1$

Table 6
Verification of RCC-MRx criteria (locations A and B).

Path name	P_m/S_m	$(P_m+P_b)/K_{eff}S_m$	$((P_m+P_b)_{Max}+\Delta Q_{Max})/3S_m$
A0_1	0.09	0.07	0.61
A0_3	0.10	0.07	0.66
A0_5	0.10	0.07	0.66
A0_7	0.09	0.07	0.64
A1_1	0.12	0.10	0.52
B0_2	0.09	0.07	0.65
B0_4	0.09	0.07	0.66
B0_6	0.09	0.07	0.65

Table 7
Verification of RCC-MRx criteria (locations C and D).

Path name	P_m/S_m	$(P_m+P_b)/K_{eff}S_m$	$((P_m+P_b)_{Max}+\Delta Q_{Max})/3S_m$
C1	0.16	0.14	0.21
C2	0.14	0.12	0.26
C3	0.16	0.14	0.24
C4	0.16	0.14	0.27
D5	0.15	0.13	0.22
D6	0.15	0.13	0.26
D7	0.16	0.15	0.28
D8	0.16	0.15	0.25

to be further investigated with more in-depth studies, once a realistic system of supports will be designed.

The equivalent Von Mises stress field arising within the FW PMU test section is reported in Fig. 15. Results show high stress values in some regions, which are mostly due to the high temperatures arising in the structure (higher than 500 °C). To this purpose, a stress linearization procedure has been performed to assess the compliance of the results with the RCC-MRx structural design codes.

Three criteria were taken into account: the Immediate Excessive Deformation (IED), the Immediate Plastic Instability (IPI) and the Ratcheting criteria and they are reported in Table 5.

In the criteria discussed above, S_m is the maximum allowable primary membrane stress intensity of the material, related to the Level of service A, while K_{eff} is the "plastic collaboration coefficient", which is equal to 1.5 for rectangular sections. The values of S_m, as functions of temperature, for EUROFER97 steel and AISI316L were drawn respectively from [8,16].

For the ratcheting criteria, the $3S_m$ rule was selected. The term $(P_m + P_b)_{Max}$ is intended as the maximum equivalent primary stress chosen between the results at $t = 0$ and $t = t_{final}$. Looking at the second addendum of the expression, the ΔP is the maximum range of stress due to disruption loading which is negligible for the FW and blanket [20]. Then, in this case only the ΔQ is considered which is equal to $(Q_m + Q_b)_{t_{final}} - (Q_m + Q_b)_0$.

The stress linearization procedure was performed along some significant paths located within the most stressed regions of the structure, which are reported in Figs. 16 and 17. To ease the comprehension, the path nomenclature is explained in Fig. 18.

The main results are reported in Tables 6 and 7.

The stress components related to the initial time of the test were calculated adopting the thermal field of Fig. 12.

The nomenclature of the selected paths was arranged by considering two YZ planes, locations A and B, in the FW structure, and other eight XY planes in the locations C and D, one for each of the eight channels, in the inlet/outlet pipes.

Regarding the paths selected within the FW structure, indices from 0 to 3 were chosen to consider the different regions of the path, reported on the right side of Fig. 18. Moreover, the last index of the path, in case of the locations A and B, from 1 to 8, represents the number of the channel (Fig. 18).

Concerning the paths selected within the FW PMU inlet/outlet pipes (pertaining to the locations C and D), the paths were chosen in the thickness of the channel (as depicted in Fig. 17) and the indices represent the number of the channel to which the manifold is connected.

For the sake of brevity, only the results relevant to the paths with values higher than 0.50 are reported in the Table 6, in case of the paths chosen in the locations A and B. Some other paths relevant to the locations C and D are reported in Table 7.

Looking at the results, all of the paths verify the criteria considered by a very wide margin. In particular, concerning the IED and IPI criteria, all the paths of the four locations fulfil the criteria with values always lower than 0.20.

For what concerns the ratcheting rule, in these cases the values are slightly higher. This happens because of the presence of the equivalent secondary stresses in the criterion. However, despite the very conservative formulation of the $3S_m$ rule, even in this case, the criterion is satisfied for all the chosen paths, with the maximum values around 0.65 in the EUROFER97 structures.

5. Conclusions

The WL facility, integrated in the W-HYDRA platform at the ENEA Brasimone research centre, will host BB components PMUs, to test their performance by assessing potential showstoppers and to collect experimental data to validate the computational methodologies to be adopted for the design of the DEMO reactor and future fusion power plants.

In this framework, the present research campaign is focussed on the preliminary study of the thermo-structural performances of the BB FW PMU test section. At first, particular attention was paid to the cooling circuit capabilities and the thermal behaviour under the normal operating conditions foreseen for the steady-state flat top experimental test. The results showed acceptable pressure drops and an even flow distribution among the FW PMU channels. Potential coolant vaporization issues may be noticed in some areas of the FW PMU, which should be addressed by means of dedicated two-phase CFD analyses. Moreover, the structure reaches high temperatures above 500 °C without overcoming the suggested limit temperature of EUROFER97.

Then, the structural thermal distribution was adopted as input data for the thermomechanical assessment. The structural behaviour of the FW PMU test section is acceptable. Looking at the examined structural design criteria, the test section presents a very good behaviour, fulfilling all the criteria by a wide range. By the way, an high maximum total displacement along the Y direction is noted, but these values may be improved with further studies, once a more realistic system of support is designed.

CRediT authorship contribution statement

F.M. Castrovinci: Writing – original draft, Methodology, Investigation, Conceptualization. **P. Arena:** Writing – original draft, Methodology, Investigation, Conceptualization. **N. Badodi:** Writing – original draft, Methodology, Investigation, Conceptualization. **G. Bongiovì:** Writing – original draft, Methodology, Investigation, Conceptualization. **I. Catanzaro:** Writing – original draft, Methodology, Investigation, Conceptualization. **A. Del Nevo:** Writing – original draft, Methodology, Investigation, Conceptualization. **P.A. Di Maio:** Writing – original draft, Methodology, Investigation, Conceptualization. **S. Giambrone:** Writing – original draft, Methodology, Investigation, Conceptualization. **P. Maccari:** Writing – original draft, Methodology, Investigation, Conceptualization. **G. Mongiardini:** Writing – original draft, Methodology, Investigation, Conceptualization. **A. Quartararo:** Writing – original draft, Methodology, Investigation, Conceptualization. **E. Vallone:** Writing – original draft, Methodology, Investigation, Conceptualization.

Declaration of competing interest

The authors declare that they have no known competing financial interests or personal relationships that could have appeared to influence the work reported in this paper.

Acknowledgements

This work has been carried out within the framework of the EUROfusion Consortium, funded by the European Union via the Euratom Research and Training Programme (Grant Agreement No 101052200 — EUROfusion). Views and opinions expressed are however those of the author(s) only and do not necessarily reflect those of the European Union or the European Commission. Neither the European Union nor the European Commission can be held responsible for them.

Data availability

Data will be made available on request.

References

[1] G. Federici, C. Bachmann, L. Barucca, W. Biel, L. Boccaccini, R. Brown, C. Bustreo, S. Ciattaglia, F. Cismondi, M. Coleman, V. Corato, C. Day, E. Diegele, U. Fischer, T. Franke, C. Gliss, A. Ibarra, R. Kembleton, A. Loving, F. Maviglia, B. Meszaros, G. Pintsuk, N. Taylor, M. Tran, C. Vorpahl, R. Wenninger, J. You, DEMO design activity in Europe: Progress and updates, Fusion Eng. Des. 136 (2018) 729–741, http://dx.doi.org/10.1016/j.fusengdes.2018.04.001, Special Issue: Proceedings of the 13th International Symposium on Fusion Nuclear Technology (ISFNT-13).

[2] P. Di Maio, P. Arena, G. Bongiovì, P. Chiovaro, R. Forte, S. Garitta, On the optimization of the first wall of the DEMO water-cooled lithium lead outboard breeding blanket equatorial module, Fusion Eng. Des. 109–111 (2016) 335–341, http://dx.doi.org/10.1016/j.fusengdes.2016.02.103, Proceedings of the 12th International Symposium on Fusion Nuclear Technology-12 (ISFNT-12).

[3] P. Di Maio, P. Arena, G. Bongiovì, I. Catanzaro, A. Del Nevo, R. Forte, On the effect of stiffening plates configuration on the DEMO water cooled lithium lead breeding blanket module thermo-mechanical behaviour, Fusion Eng. Des. 146 (2019) 2247–2250, http://dx.doi.org/10.1016/j.fusengdes.2019.03.163.

[4] I. Catanzaro, P. Arena, S. Basile, G. Bongiovì, P. Chiovaro, A. Del Nevo, P.A. Di Maio, R. Forte, I.A. Maione, E. Vallone, Structural assessment of the EU-DEMO WCLL central outboard blanket segment under normal and off-normal operating conditions, Fusion Eng. Des. 167 (2021) 112350, http://dx.doi.org/10.1016/j.fusengdes.2021.112350.

[5] I. Catanzaro, G. Bongiovì, P. Di Maio, P. Arena, G. Spagnuolo, Structural assessment of the EU-DEMO water-cooled lead lithium central outboard blanket segment adopting the sub-modelling technique, Fusion Eng. Des. 192 (2023) 113601, http://dx.doi.org/10.1016/j.fusengdes.2023.113601.

[6] S. Giambrone, P. Arena, G. Bongiovì, I. Catanzaro, A. Del Nevo, P. Di Maio, E. Tomarchio, E. Vallone, S. Basile, Study of the thermo-mechanical performances of the EU-DEMO water-cooled lead lithium left outboard blanket segment, Fusion Eng. Des. 192 (2023) 113837, http://dx.doi.org/10.1016/j.fusengdes.2023.113837.

[7] P. Arena, A.D. Nevo, M. Eboli, B. Gonfiotti, P. Maccari, R. Marinari, A. Tincani, N. Badodi, G. Bongiovì, I. Catanzaro, F. Galleni, C. Risi, L. Sanasi, A. Tarallo, A. Vannoni, W-HYDRA: a new experimental platform for the water-cooled lead lithium breeding blanket, Nucl. Fusion 64 (7) (2024) 076043, http://dx.doi.org/10.1088/1741-4326/ad50e9.

[8] RCC-MRx, Design and Construction Rules for Mechanical Components of Nuclear Installations, Afcen, 2012.

[9] P. Arena, G. Bongiovì, I. Catanzaro, C. Ciurluini, A. Collaku, A. Del Nevo, P.A. Di Maio, M. D'Onorio, F. Giannetti, V. Imbriani, P. Maccari, L. Melchiorri, F. Moro, R. Mozzillo, S. Noce, L. Savoldi, S. Siriano, A. Tassone, M. Utili, Design and integration of the EU-DEMO water-cooled lead lithium breeding blanket, Energies 16 (4) (2023) http://dx.doi.org/10.3390/en16042069.

[10] P. Maccari, P. Arena, R. Marinari, A. Tincani, A. Del Nevo, Design of a prototypical mock-up for the experimental investigation of WCLL first-wall performances, Energies 16 (4) (2023) http://dx.doi.org/10.3390/en16041685.

[11] I. Catanzaro, G. Bongiovì, P.A. Di Maio, Analysis of the thermo-mechanical behaviour of the EU DEMO water-cooled lithium lead central outboard blanket segment under an optimized thermal field, Appl. Sci. 12 (3) (2022) http://dx.doi.org/10.3390/app12031356.

[12] F.A. Hernández, P. Arena, L.V. Boccaccini, I. Cristescu, A. Del Nevo, P. Sardain, G.A. Spagnuolo, M. Utili, A. Venturini, G. Zhou, Advancements in designing the DEMO driver blanket system at the EU DEMO pre-conceptual design phase: Overview, challenges and opportunities, J. Nucl. Eng. 4 (3) (2023) 565–601, http://dx.doi.org/10.3390/jne4030037.

[13] F. Gillemot, et al., Material property handbook pilot project on EUROFER97 (MTA EK, KIT), 2016, EUROfusion IDM Ref.: 2MRP77.

[14] ANSYS Inc., ANSYS CFX-Solver Theory Guide, 2021, Release: 2021 R2.

[15] International Association for the Properties of Water and Steam, Revised release on the IAPWS industrial formulation 1997 for the thermodynamic properties of water and steam, 2007.

[16] The American Society of Mechanical Engineers, Boiler and pressure vessel code, section II - part D, 2015.

[17] P.J. Linstrom, W.G. Mallard (Eds.), NIST Chemistry WebBook, NIST Standard Reference Database Number 69, National Institute of Standards and Technology, Gaithersburg MD, 20899, http://dx.doi.org/10.18434/T4D303, (Retrieved September 9, 2019).

[18] L.S. Tong, A phenomenological study of critical heat flux ASME paper 75-HT-68, 1975.

[19] T. Haertl, C. Bachmann, E. Diegele, G. Federici, Rationale for the selection of the operating temperature of the DEMO vacuum vessel, Fusion Eng. Des. 146 (2019) 1096–1099, http://dx.doi.org/10.1016/j.fusengdes.2019.02.014.

[20] X. Wang, X. Wang, Z. Li, J. Chen, Assessment of the structural design criteria to prevent ratcheting damage for fusion component design, Fusion Eng. Des. 171 (2021) 112660, http://dx.doi.org/10.1016/j.fusengdes.2021.112660.